TENTH AUSTRALASIAN FLUID MECHANICS
CONFERENCE - UNIVERSITY OF MELBOURNE
11-15 DECEMBER 1989

SHEAR STRESS PROFILES IN ZERO-PRESSURE-GRADIENT TURBULENT BOUNDARY LAYERS

J.D. LI and A.E. PERRY

Department of Mechanical Engineering
University of Melbourne, Parkville, Vic. 3052
AUSTRALIA

ABSTRACT

Analytical expressions are derived for the Reynolds shear stress profiles in zero pressure gradient boundary layers. Some of the properties of these profiles have been discussed and comparisons are made with hot-wire data.

1. INTRODUCTION

There has always been the need for some reliable analytical expressions of Reynolds shear stress profiles in turbulent boundary layers. Such expressions could be used for the study of conditions necessary for equilibrium flows, for the checking of hot-wire anemometer measurements and for cross checking the skin friction estimation made by other methods, particularly on rough walls. Analytical expressions could guide us in developing a procedure for extrapolating measured shear stress data to the wall. In this paper, Coles' velocity profile (1956, 1962 and 1969) has been modified to apply to the whole boundary layer beyond the buffer zone. The analytical expressions for the Reynolds shear stress profiles in smooth and rough wall zero pressure gradient turbulent boundary layers are then derived. Many people have attempted a similar task, among them, Coles (1952), Tetervin & Lin (1955), Townsend (1956), Coles (1957) and Rotta (1962), all with some simplifying assumptions. Perry (1968) presented a detailed analysis of the shear stress profiles using the law of the wall and the one parameter velocity defect profile family. Some of the results concerning the zero pressure gradient flows on both the smooth and 'd-type' rough walls have been given in Li, Henbest & Perry (1986). Granville (1988) also derived the shear stress profiles for smooth and rough walls in zero pressure gradient flows using a different strategy, but his analysis cannot be applied to the 'd-type' rough wall. The analytical results are then compared with the experimental results and show good agreement. Some of the discrepancies have been explained. Similar work has also been done by the authors on arbitrary pressure gradient boundary layers and the results will be published later.

Coles' velocity formula (1956, 1962 and 1969) on smooth walls

$$\frac{U}{U_\tau} = \frac{1}{\kappa}\ln\frac{zU_\tau}{\nu} + A + \frac{\Pi}{\kappa}w(\frac{z}{\delta_c}) \qquad (1)$$

is assumed throughout this paper. Here U is the local mean streamwise velocity, U_τ the wall shear velocity, z the distance from the wall, κ the Kármán constant, ν the kinematic viscosity, A a universal constant, Π the wake strength, $w(z/\delta_c)$ the wake function and δ_c is Coles' boundary layer thickness.

2. MODIFICATION OF COLES' FORMULA

Hinze (1959) suggested the functional form for $w(z/\delta_c)$ in equation (1) as,

$$w(\frac{z}{\delta_c}) = 1 - \cos(\pi\frac{z}{\delta_c}) \qquad (2).$$

It is a well known fact that the velocity derivative $\partial U/\partial z$ of Coles' velocity profiles (1) and (2) is not zero at $z = \delta_c$. In order to overcome this problem, a factor β is introduced into equation (2) and the velocity profile beyond the buffer zone is,

$$\frac{U}{U_\tau} = \frac{1}{\kappa}\ln\frac{zU_\tau}{\nu} + A + \frac{\Pi}{\kappa}(1 - \cos(\beta\pi\frac{z}{\delta_H})) \qquad (3)$$

Here $\delta_H = \delta^* U_1/C_1U_\tau$ where δ^* is the displacement thickness, U_1 the freestream velocity and C_1 is a constant which will be defined later (after equ. 14). The factor β is found from,

$$1 + \Pi\beta\pi\sin(\beta\pi) = 0 \qquad (4).$$

It can be seen that $\beta \to 1$ as $\Pi \to \infty$ and $\beta = 1.1654$ at $\Pi = 0.55$, which is the value suggested by Coles as the asymptotic value when the Reynolds number is above $R_\theta = 6000$. The geometric meaning of β is $\delta_H = \beta\,\delta_c$ and the defect law after inserting the factor β in is,

$$\frac{U_1 - U}{U_\tau} = -\frac{1}{\kappa}\ln(\frac{z}{\delta_H}) + \frac{\Pi}{\kappa}(-\cos(\beta\pi) + \cos(\beta\pi\frac{z}{\delta_H})) \qquad (5).$$

3. SHEAR STRESS PROFILES ON ZERO PRESSURE GRADIENT SMOOTH WALLS

Figure 1 shows the various definitions of the quantities used below. It is assumed that the velocity profile in a boundary layer can be described by a viscous zone and an outer flow region. In the viscous zone, it is assumed that:

$$\frac{U}{U_\tau} = f_s(\xi) \qquad (6)$$

where $\xi = z/z_0$, $z_0 = M\nu/U_\tau$ and M is a constant around 50 for smooth wall turbulent boundary layers.

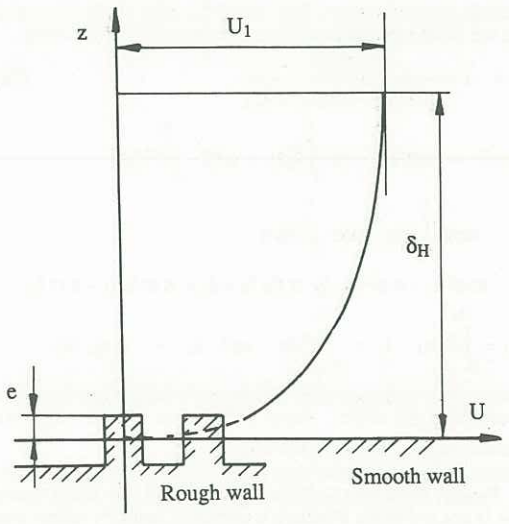

Figure 1 The various definitions used in boundary layer.

In the outer flow region the velocity profile is given as,

$$\frac{U_1 - U}{U_\tau} = f(\eta, \Pi) \quad (7)$$

where $\eta = z/\delta_H$. Using the boundary layer approximation and assuming two-dimensional flow, the mean momentum and continuity equations are,

$$U\frac{\partial U}{\partial x} + W\frac{\partial U}{\partial z} = \frac{1}{\rho}\frac{\partial \tau}{\partial z} \quad (8)$$

$$\frac{\partial U}{\partial x} + \frac{\partial W}{\partial z} = 0 \quad (9)$$

where $\tau/\rho = \nu\,\partial U/\partial z - \overline{uw}$ is the total shear stress and $-\overline{uw}$ is the Reynolds shear stress. The boundary conditions are,

$$U = W = 0,\ \tau = \tau_0 \text{ at } z = 0 \quad (10a)$$

$$U = U_1,\ \tau = 0 \text{ at } z = \delta_H \quad (10b).$$

The normal to the wall mean velocity W can be found from equation (9). Substituting W and the velocity profile (7) into equation (8) gives,

$$\left(\frac{d\delta_H}{dx}\right)^{-1}\frac{\partial \tau/\tau_0}{\partial \eta} = -\sigma\Phi f + \sigma\eta f' + \Phi f^2 + \Phi\eta_0 f_s(1) f' - \Phi f' \int_{\eta_0}^{\eta} f d\eta - f' \int_{\eta_0}^{\eta} f d\eta - \eta_0 f_s(1) f' \quad (11)$$

where $\sigma = \frac{U_1}{U_\tau}$, $\Phi = \frac{1}{U_\tau}\frac{dU_\tau}{dx}\left(\frac{1}{\delta_H}\frac{d\delta_H}{dx}\right)^{-1}$, $f' = \partial f/\partial\eta$ and $\eta_0 = z_0/\delta_H$. After substituting the boundary condition $U = U_1$ at $z = \delta_H$, equation (3) becomes,

$$\sigma = \frac{U_1}{U_\tau} = \frac{1}{\kappa}\ln\frac{\delta_H U_\tau}{\nu} + A + \frac{\Pi}{\kappa}(1 - \cos(\beta\pi)) \quad (12).$$

By differentiating equation (12), Φ can be obtained as,

$$\Phi = -\frac{1}{\kappa\sigma + 1} \quad (13).$$

Using the definition for the momentum thickness θ, it can be shown that:

$$\frac{\theta}{\delta_H} = \frac{C_1}{\sigma} - \frac{C_2}{\sigma^2} \quad (14)$$

where $C_1 = \int_0^1 f d\eta$ and $C_2 = \int_0^1 f^2 d\eta$. In deriving equation (14), the velocity defect profile (7) has been used and the sublayer effect has been neglected according to Perry (1968). Combining the momentum integral equation $d\theta/dx = 1/\sigma^2$ and equations (13) & (14), it can be shown that,

$$\frac{d\delta_H}{dx} = \frac{\kappa\sigma + 1}{\kappa\sigma^2 C_1 - \kappa\sigma C_2 + C_2} \quad (15).$$

Substituting equations (13) and (15), after integration and using the boundary condition (10), equation (11) becomes,

$$\frac{\tau}{\tau_0} = 1 + \frac{C+D}{\kappa\sigma^2 C_1 - \kappa\sigma C_2 + C_2} \quad (16)$$

where $C = \kappa\sigma^2\eta f - \kappa\sigma^2\int_0^\eta f d\eta + \sigma\eta f - \int_0^\eta f^2 d\eta - \kappa\sigma f\int_0^\eta f d\eta + \kappa\sigma\int_0^\eta f^2 d\eta$

$D = \kappa\sigma^2 I_1 - \kappa\sigma^2\eta_0 f_0 - \sigma\eta_0 f_0 + I_2 + \kappa\sigma f_0 I_1 - \kappa\sigma I_2$

and $I_1 = \int_0^{\eta_0} f d\eta$, $I_2 = \int_0^{\eta_0} f^2 d\eta$ and $f_0 = f(\eta_0, \Pi)$.

The term D in equation (16) represents a correction from the viscous sublayer effect, Perry (1968) has shown that this correction can be neglected for $\sigma \geq O(10)$.

There are some interesting features concerning equation (16). Firstly, as Rotta (1962) has pointed out, the shear stress profile is not universal although a universal velocity defect law is used in deriving equation (16). From dimensional analysis, combined with the momentum equation, Rotta concluded that equilibrium of the turbulent boundary layer on a flat plate can be reconciled with the flow equations only if $\sigma = \sqrt{2/C_f'}$ is a constant and this would be achieved if the plate were covered with a 'k-type' roughness distribution continuously varying in such a manner that the representative length scale of the roughness is everywhere in constant ratio to the distance x from the leading edge. Secondly, since σ approaches infinity as the Reynolds number approaches infinity, the above expression for shear stress can be simplified for infinite Reynolds number as,

$$\frac{\tau}{\tau_0} = 1 + \frac{f\eta - \int_0^\eta f d\eta}{C_1} \quad (17)$$

which is a universal function of η. Note also that the shear stress gradient in the turbulent wall region is not zero when the Reynolds number approaches infinity but is given by,

$$\frac{\partial \tau/\tau_0}{\partial \eta} = -\frac{1}{\kappa C_1} \quad (18).$$

Thus according to equations (17) and (18), the turbulent wall region is not a region of constant shear stress. Equation (18) was first given by Perry (1968) and first stated in the open literature by Li *et al.* (1986). Spalart (1988) independently arrived at the same result.

Another interesting point about equation (16) is the slope of the shear stress in the turbulent wall region at low Reynolds numbers. It was generally believed that this slope should be zero, but calculations using equation (16) show that it is finite. Spalart (1988), by using a supercomputer, has carried out a full direct simulation of a flat plate turbulent boundary layer and found that from $R_\theta = 667$ to 1410, the total shear stress profiles have finite slopes in the turbulent wall region. This is consistent with the present analysis.

The Reynolds shear stress after taking into account direct viscous effect is calculated as follows,

$$\frac{-\overline{uw}}{U_\tau^2} = \frac{\tau}{\tau_0} - \frac{1}{K_\tau}\frac{\partial U/U_\tau}{\partial \eta} \quad (19)$$

where $K_\tau = U_\tau\delta_H/\nu$ and will be referred to as the Kármán number.

Figure 2 shows the calculated Reynolds shear stress profiles using equations (19) and (16) for various Reynolds numbers, with the velocity profile (5) being used. Figure 2 shows that the maximum value for Reynolds shear stress at $R_\theta = 10^3$ is about 0.9. This agrees well with the supercomputer results of Spalart (1988) and the experimental data of Erm, Smits & Joubert (1986). In the near wall region, the Reynolds shear stresses approach the universal profile (17) monotonically as the Reynolds number increases. At very high Reynolds number, the Reynolds shear stress approaches 1 close to the wall. However, at $z/\delta_H = 0.1$, the highest

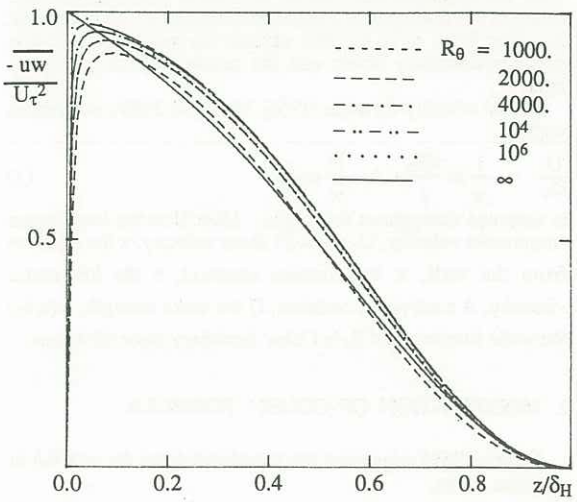

Figure 2 The Reynolds shear stress profiles on smooth wall calculated from equations (16) and (19) with P values chosen according to Coles (1962).

attainable Reynolds shear stress is about 0.95 rather than the generally believed value of 1.

4. SHEAR STRESS PROFILES ON ZERO PRESSURE GRADIENT ROUGH WALLS

The general velocity profile expression on rough walls is,

$$\frac{U}{U_\tau} = \frac{1}{\kappa}\ln\left(\frac{zU_\tau}{\nu}\right) + A - \frac{\Delta U}{U_\tau} + \frac{\Pi}{\kappa}(1 - \cos(\beta\pi\eta)) \qquad (20)$$

where $\Delta U/U_\tau$ is the roughness function and is a function of hU_τ/ν. Here h is the effective roughness scale.

Experimental data have shown that when hU_τ/ν is sufficiently large, $\Delta U/U_\tau$ itself is a logarithmic function of hU_τ/ν. Perry, Schofield & Joubert (1969) have pointed out that there are two kinds of rough walls. One is called the 'k-type' rough wall and the other the 'd-type' rough wall. On 'k-type' rough walls,

$$\frac{\Delta U}{U_\tau} = \frac{1}{\kappa}\ln\frac{kU_\tau}{\nu} + K \qquad (21)$$

where the effective roughness scale h is proportional to the length scale of the roughness element k and K is a characteristic constant of roughness. On 'd-type' rough walls,

$$\frac{\Delta U}{U_\tau} = \frac{1}{\kappa}\ln\frac{\delta_H U_\tau}{\nu} + D \qquad (22)$$

where the effective roughness scale h is proportional to the boundary layer thickness δ_H and D is a characteristic constant of roughness. On rough walls, we assume that the defect law formula (7) is valid down to the crests of the roughness elements and $\eta_0 = e/\delta_H$ corresponds to the roughness element crests.

4.1 'k-type' Rough Wall

The procedure of deriving the shear stress profiles on rough walls is the same as on smooth walls. It can be shown that,

$$\left(\frac{d\delta_H}{dx}\right)\frac{\partial\tau/\tau_0}{\partial\eta} = -\sigma\Phi f + \sigma\eta f' + \Phi f^2 - \Phi f'\int_{\eta_0}^{\eta} f\,d\eta - f'\int_{\eta_0}^{\eta} f\,d\eta - \eta_0 f_0 f' \qquad (23).$$

Using equations (20) and (21), after substituting $z = \delta_H$, one obtains,

$$\Phi = -\frac{1}{\kappa\sigma} \qquad (24)$$

for 'k-type' rough walls. By integrating (23) and using the boundary condition (10), one has,

$$\frac{d\delta_H}{dx} = \frac{\kappa\sigma}{E} \qquad (25)$$

where $E = \kappa\sigma^2(C_1 - I_1) - \sigma(C_1 - I_1) + 2(C_2 - I_2) - \kappa\sigma(C_2 - I_2) + \kappa\sigma\eta_0 f_0(\sigma - f_0)$.

The shear stress profile after integrating equation (23) is,

$$\frac{\tau}{\tau_0} = 1 + \frac{F}{E} \qquad (26)$$

where $F = \kappa\sigma^2(\eta f - \eta_0 f_0) - \kappa\sigma^2\left(\int_0^{\eta} f\,d\eta - I_1\right) + \sigma\left(\int_0^{\eta} f\,d\eta - I_1\right) - \kappa\sigma\eta_0 f_0(f - f_0) + f\left(\int_0^{\eta} f\,d\eta - I_1\right) - 2\left(\int_0^{\eta} f^2 d\eta - I_2\right) - \kappa\sigma f\left(\int_0^{\eta} f\,d\eta - I_1\right) + \kappa\sigma\left(\int_0^{\eta} f^2 d\eta - I_2\right)$

As $\delta_H/k \to \infty$, $\eta_0 \to 0$ and $I_1 = I_2 = 0$, expression (26) is the same as equation (17).

4.2 'd-type' Rough Wall

For 'd-type' rough wall, the analysis will be simpler since σ = constant according to Perry *et al.* (1969). The expression for $\partial(\tau/\tau_0)/\partial\eta$ will be the same as equation (23) and from equations (20) and (22), it can be shown that,

$$\Phi = 0 \qquad (27)$$

and $$\frac{d\delta_H}{dx} = \frac{1}{H} \qquad (28)$$

where $H = \sigma C_1 - C_2 + \sigma\eta_0 f_0 - \sigma I_1 - \eta_0 f_0^2 + I_2$. The shear stress profile is,

$$\frac{\tau}{\tau_0} = 1 + \frac{M}{H} \qquad (29)$$

where $M = \sigma(\eta f - \int_0^{\eta} f\,d\eta) - \eta_0 f_0 f - (f\int_0^{\eta} f\,d\eta - \int_0^{\eta} f^2 d\eta) - \sigma(\eta_0 f_0 - I_1) + \eta_0 f_0^2 + (fI_1 - I_2)$.

Because σ = const. on 'd-type' rough walls, the expression (29) is self-preserving and therefore we have equilibrium flow. For small η_0 and large σ, equation (29) reduces to the universal equilibrium form as given by equation (17).

5. THE EXPERIMENTAL REYNOLDS SHEAR STRESS RESULTS

5.1 Smooth Wall Results

In all the experimental boundary layers mentioned here, great care was taken to ensure minimum three dimensionality of the mean flows. Spanwise distributions of V were found to be small confirming the absence of secondary flow. The Reynolds shear stresses on smooth walls were measured using a 90^0 stationary X-wire. The measured Reynolds shear stresses are non-dimensionalized using the U_τ^2 values obtained from the Preston tube method and are shown in figure 3. Also shown in the figure are the calculated Reynolds shear stress profiles according to equations (16) and (19) for the corresponding lowest and highest Reynolds numbers as well as the infinite Reynolds number case. The wake strength parameters for calculating the profiles were chosen according to the mean flow results at finite Reynolds numbers and is 0.55 at infinite Reynolds number.

Figure 3 shows that the experimental results agree reasonably well with the calculated results except in the near wall region. One of the reasons for this discrepancy might be due to the velocity gradient along the wires as suggested by Lawn (1971). Another possibility is due to the spatial resolution effect. The data from Ligrani, Westphal & Lemos (1987) using a subminiature hot-wire probe together with a standard size probe clearly show that spatial resolution has an effect on the streamwise, the normal to the wall broadband turbulent intensities and the Reynolds shear stress. Unfortunately, we do not know how to correct this spatial resolution effect for Reynolds shear stress so far. Due to the present experimental errors involved, it is felt that the agreement between the experimental and the calculated

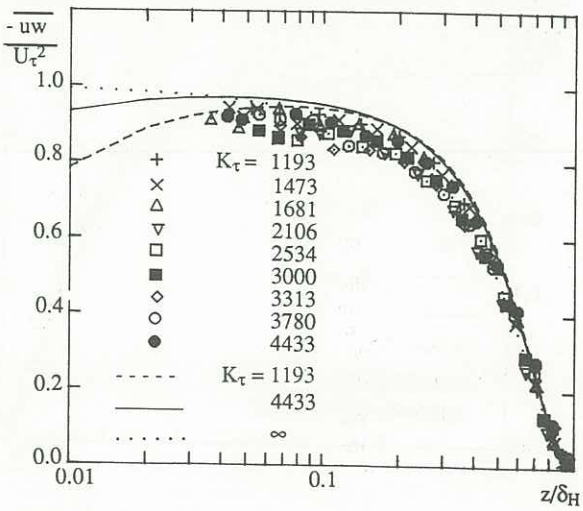

Figure 3 The measured Reynolds shear stress results on smooth wall.

Reynolds shear stress results shown in figure 3 is acceptable.

5.2 Rough Wall Results

Figure 4 shows the measured Reynolds shear stress results for the 'k-type' rough wall and the corresponding calculation from the above theory. The experimental results were non-dimensionalized by the U_τ^2 values obtained from the method outlined in Li (1989).

As discovered by Perry, Lim, Henbest & Chong (1983), a stationary 90^0 X-wire probe will suffer a 'cone angle' problem over the 'k-type' rough wall and the way to overcome this is by either 'flying' the wire and/or using a 120^0 X-wire probe. Figure 4 shows that the 120^0 wire probe and the 'flying' wires improve the Reynolds shear stress results for the 'k-type' rough wall and agree with each other quite well. Figure 4 also shows that the present 'flying' hot-wire and 120^0 X-wire results agree very well with the theoretically calculated ones for 'k-type' rough wall.

Over the 'd-type' rough wall, it is known from Perry *et al.* (1969) that a 'precise' equilibrium layer exists and the momentum thickness θ increases linearly from some starting position. Thus the wall shear stress can be derived from $d\theta/dx$ without suffering serious discrete point differentiation inaccuracies. This might be true when the Reynolds number is high. In the present 'd-type' rough wall experiment, since the Reynolds number is low, the extrapolation method of inferring wall shear stress using the Reynolds shear stress profile (Li *et al.*, 1986) is used to obtain the U_τ values instead of the $d\theta/dx$ method. Figure 5 shows the Reynolds shear stress results measured over the 'd-type' rough wall using the 90^0 stationary X-wire and non-dimensionalized using U_τ^2 values obtained by the extrapolation method. The U_τ values obtained this way are between the values obtained using the $d\theta/dx$ method and the mean velocity similarity method mentioned in Li (1989) and is less than 3% different from the U_τ values obtained by both methods.

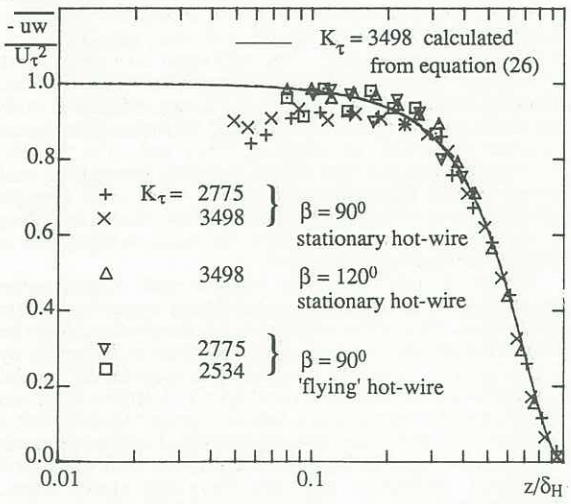

Figure 4 The measured Reynolds shear stress results on 'k-type' rough wall.

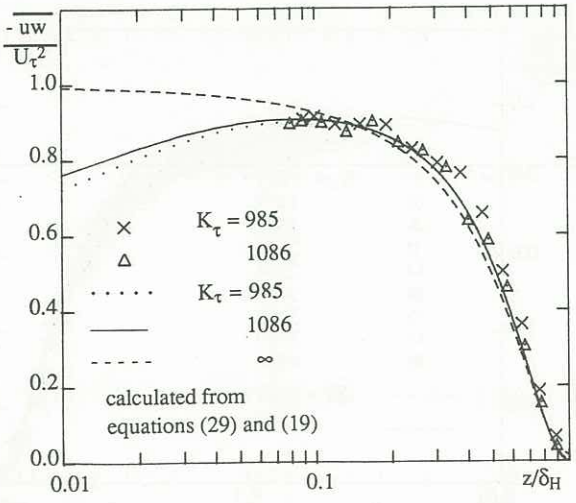

Figure 5 The measured Reynolds shear stress results on 'd-type' rough wall.

6. CONCLUSIONS AND DISCUSSION

Coles' velocity profile (1956, 1962 and 1969) has been modified and applied to the whole boundary layer beyond the viscous sublayer. The derived shear stress profiles in zero pressure gradient turbulent boundary layers show the Reynolds number effect as mentioned by Townsend (1956) and Rotta (1962), i.e. a universal shear stress profiles can be achieved only when the Reynolds number approaches infinity. This universal shear stress profile has been discussed by Perry (1968) and shows a striking feature in that its slope is finite in the turbulent wall region. The general analytical Reynolds shear stress profiles have been compared with the experimental data and encouraging agreement has been found. Further work is needed to investigate the discrepancy between the theoretical results and the experimental ones on the smooth wall. Although many people belive that spatial resolution should not be a problem for the Reynolds shear stress, the recent investigation by Ligrani *et al.* (1987) has shown that this may not be true. Hence some method is needed to correct this effect.

The authors wish to thank the Australian Research Council for the financial support of this project.

REFERENCE

COLES, D. 1952 *In Jahre Grenzschicht-forschung*, ed Gortler, H. & Tollmien, W., pp.153-163. Vieweg: Braunschweig.

COLES, D. 1956 *J. Fluid Mech.* **1**, pp.191-226.

COLES, D. 1957 *J. Aero. Sci.* **24**, pp.495-506.

COLES, D. 1962 *U.S.A.F. The Rand Cooperation, Report R-403-PR*, Appendix A.

COLES, D. 1969 *Proc. 1968 AFOSR-IFP Stanford Conference on Comput. of Turb. Boundary-Layers.* **2**, PP.1-45.

ERM, L.P., SMITS, A.J. & JOUBERT, P.N. 1986 *Turbulent Shear Flow* (ed. Durst, F., Launder, B.E., Lumley, J.L., Schmidt, F.W. & Whitelaw, J.H.), **5**, Springer-Verlag.

GRANVILLE, P. S. 1988 *J. Ship Res.*, **32** No.4 pp.229-237.

HINZE, J.O. 1959 Turbulence McGraw-Hill, New York.

LAWN, C.J. 1971 *J. Fluid Mech.* **48**, part 4, pp.477-505.

LI, J.D. 1989 Ph.D. thesis University of Melbourne, Australia.

LI, J.D., HENBEST, S.M & PERRY, A.E. 1986 *Proc. 9th Australasian Fluid Mech. Conf.*, Auckland, New Zealand.

LIGRANI, P. M., WESTPHAL, R. V. & LEMOS, F. R. 1987 *NASA Tech. Mem.*

PERRY, A.E. 1968 'Equilibrium Boundary Layer', *Unpublished.*

PERRY, A.E., LIM, K.L., HENBEST, S.M. & CHONG, M.S. 1983 *Proc. 4th Intl. Symposium on Turb. Shear Flow*, Karlsruhe, W. Germany.

PERRY, A.E., SCHOFIELD, W.H. & JOUBERT, P.N. 1969 *J. Fluid Mech.* **37**, part 2, pp.381-413.

ROTTA, J.C. 1962 *Progress in Aero.* **2**, Pergammon Press.

SPALART, P.R. 1988 *J. Fluid Mech.* **187**, pp.61-98.

TETERVIN, N. & LIN, C.C. 1955 *NASA Report* p.1046.

TOWNSEND, A.A. 1956 The Structure of Turbulent Shear Flow Cambridge University Press.